Circulating tumour DNA is a potential biomarker for disease progression and response to targeted therapy in advanced thyroid cancer

Allin DM, Shaikh R, Carter P, Thway K, Gonzales-de-Castro D, O'Leary B, Garcia-Murillas I, Hubank M, Harrington K, Kim D, Newbold K

ABSTRACT

BACKGROUND

Conventional biomarkers in thyroid cancer (thyroglobulin, calcitonin, CEA) are not disease-specific and can fluctuate in advanced disease, making interpretation difficult. Cell-free circulating tumour DNA (ctDNA) has been shown to be a useful biomarker in other solid tumours. We hypothesized that ctDNA is a potential candidate for a disease-specific, minimally invasive biomarker with the potential to guide personalised treatment plans in thyroid cancer. This proof-of-concept study was a multi-mutational analysis of ctDNA to test this hypothesis in patients with advanced thyroid cancer over multiple time-points.

METHODS

Mutational analysis of archival tumour tissue was performed on an NGS platform using a validated gene panel targeted to known cancer hotspots. Custom Taqman assays for discovered variants were designed for plasma ctDNA testing using digital droplet PCR. Concentrations of detected ctDNA were correlated with conventional biomarker concentration and axial imaging status defined by RECIST criteria.

RESULTS

Tumours were obtained from 51 patients, with the following histologies: 17 papillary, 15 follicular, 15 medullary, 3 poorly differentiated and 1 anaplastic. Variants were detected in 42 (82%) of the tumour tissue samples. Detected rates of variants in genes per histological subtype were broadly in line with published data. Plasma was assayed for ctDNA in 190 samples from 42 patients. ctDNA was detected in 67% of tested patients. Earlier detection of disease progression was noted in 2 patients with medullary thyroid cancer (MTC). In a further 2 cases, conventional biomarkers were not detected due to anti-thyroglobulin antibodies and de-differentiated disease, yet ctDNA was detected and also showed increasing levels prior to radiologically-confirmed disease progression. Changes in ctDNA concentration were noted to occur earlier than for conventional markers in response to disease progression in multiple patients receiving targeted therapies, raising the possibility that these patients might have been spared from ongoing ineffective, toxic therapy.

CONCLUSION

Detectable levels of ctDNA were found in the plasma of the majority of patients with advanced thyroid cancer. Sub-analysis suggests that ctDNA measurement may offer superiority over conventional markers in several clinically relevant scenarios. These include earlier detection of progression in MTC; use as an alternative biomarker when conventional markers are not available due to auto-antibodies or de-differentiated disease; and more rapid assessment of disease status in response to targeted therapies, thereby potentially allowing prompter discontinuation of futile therapies. These early results support the hypothesis that ctDNA may be a clinically useful biomarker in thyroid cancer and this will be tested in a planned multi-centre study.

INTRODUCTION

Serum thyroglobulin (Tg) concentration is used as a biomarker in differentiated thyroid cancer (DTC) for detection of residual thyroid tissue, persistent disease and relapse. However, it has several drawbacks that limit its clinical utility. Detection of thyroglobulin in plasma is tissue-specific, not cancer-specific, and its secretion by both benign and malignant tissue reduces its specificity. In addition, thyroglobulin levels do not accurately represent tumour burden in circumstances when anti-Tg auto-antibodies are present, affecting up to 25% of patients (1, 2), or in de-differentiated carcinoma. Furthermore, Tg is more difficult to interpret as a biomarker in patients treated with lobectomy or who have not undergone radio-iodide ablation. In medullary thyroid cancer (MTC), calcitonin and carcinoembryonic antigen (CEA) are used as alternative biomarkers. These are also not cancer-specific and can be slow to reflect changes in disease status.

Serial imaging is likewise used for monitoring and detection of disease progression. However, small volume changes may not be readily visible on anatomical or functional imaging, which can lead to a significant lag time in detecting progression. CT scanning, a frequently used modality, leads to repeated exposure of patients to ionising radiation which, in patients with a relatively indolent disease, is an important consideration. There is also an associated financial cost of serial imaging.

Given these limitations, new biomarkers are required to assist in the clinical management of thyroid cancer. A biomarker that could detect progression earlier with a high degree of specificity would be extremely useful. One that better identifies aggressive subtypes, detects recurrence at an earlier time-point and predicts response to therapies would be especially desirable.

Technological advances in genomics, such as next-generation sequencing (NGS) and digital Polymerase Chain Reaction (dPCR), allow detection of sequence-specific DNA at extremely low concentrations within clinically appropriate time and cost constraints. These advances paved the way for circulating tumour DNA (ctDNA) to emerge as a viable cancer biomarker. There is now substantial evidence of clinical utility in a variety of cancers (3-5) and, in fact, one ctDNA assay has received regulatory approval for use in the detection of an EGFR variant in non-small cell lung cancer (6). Although the exact mechanisms by which ctDNA enters the circulation are poorly described, it likely originates from either leakage from cells undergoing necrosis and apoptosis or active secretion (7-9).

Using ctDNA as a biomarker has several potential advantages. Detection of oncogenic mutations renders its presence in plasma extremely specific for cancer cells compared to conventional biomarkers. Traditional solid tumour biopsies may present DNA that is not fully representative of the mutational landscape due to intra-tumour heterogeneity (10-12). In contrast, ctDNA may provide a more complete representation of the mutational landscape present across the entirety of the patient's disease burden. Obtaining tumour tissue for DNA extraction is not always possible and may be associated with significant risk, whereas ctDNA is extracted from plasma samples at almost no risk to the patient.

A small study focussing on colorectal cancer (13) highlighted the potential use of ctDNA to identify patients with residual micro-metastatic disease after surgery. There has since been a drive towards establishing detection of ctDNA levels as a biomarker for molecular residual disease (MRD) in patients following primary treatment. There is now mounting evidence to support this approach,

using ctDNA as a “test of cure” in early solid, non-metastatic cancers in several tissues including breast (3), colon (14) and lung (15, 16).

Recent studies have shown that ctDNA is detectable in thyroid cancers of different subtypes (17-21) but have examined only a single variant or a single time point. With this in mind, the hypothesis of this study was that ctDNA, if detectable, would prove to be a predictive and prognostic biomarker for thyroid cancer, permitting individualisation of treatment. The primary aim of this proof-of-concept study was to conduct a comprehensive, multi-mutational analysis in ctDNA across a range of thyroid cancer subtypes over multiple time points. Secondary aims were to correlate changes in ctDNA concentration with currently used biomarkers (Tg, Calcitonin, CEA) and CT imaging, with the ultimate goal of generating evidence that ctDNA detected disease progression either earlier or more reliably than current biomarkers.

METHODS

Ethical Approval

Patients were recruited by the senior author (KN) from a thyroid cancer clinic at The Royal Marsden Hospital between December 2015 and September 2016. This study received approvals from the institutional review board (CCR4343) and the West of Scotland Research Ethics Service (WoSRES) committee (15/WS/0148). All patients provided written, informed consent.

Study design

Archival tumours were sequenced using an NGS platform for genetic variant discovery. Time between tumour excision and study entry is shown for each patient in supplementary table 1. Plasma samples were collected from patients at baseline, and 3-monthly thereafter. Results obtained from the tissue NGS sequencing were used to guide the design of bespoke digital droplet PCR (ddPCR) assays for detection of the identified variants in the plasma cell-free DNA (cfDNA). Analysis of the plasma cfDNA with the appropriate ddPCR assay allowed the variant(s) to be identified and to be tracked sequentially over time.

DNA extraction – Tumour

Archival formalin-fixed, paraffin-embedded (FFPE) tissue blocks were used for extraction where possible. If FFPE blocks were not available, then haematoxylin and eosin-stained (H&E) slides were used as an alternative. From the FFPE blocks, six slides were cut by microtome: one H&E slide was reviewed by a specialist pathologist to identify the tumour and comment on cellularity and tumour content, and five 10 µM non-stained slides were used for DNA extraction. Non-stained slides were de-waxed using established protocols. The H&E slide was used as a guide for manual macro-dissection of tissue from the non-stained slides. DNA was extracted using a spin column-based nucleic acid purification kit (Qiagen QIAamp DNA FFPE kit, Qiagen, Hilden, Germany). DNA clean-up was performed on samples with a concentration of <5 ng/µL using a DNA clean and concentrator kit (Zymo Research, CA, USA).

Library preparation

Library preparation was performed using the KAPA HyperPlus kit (Roche, Switzerland). DNA sample concentrations were quantified using a Qubit Fluorometer (ThermoFisher, Massachusetts, USA). The input amount of DNA per sample was 200 ng if the extracted sample concentration was >5 ng/µL with an average peak fragment size of >1000 b.p. length. If the average peak fragment size was <1000 b.p., then 400 ng was used to account for the higher fragmentation. When extracted DNA concentration did not allow for the approach described above, then a low input (50 ng) protocol was

used. Dual size selection and short-cycle amplification clean-up were performed using AMPure XP clean-up beads (Beckman Coulter, Brea, CA, USA). Library amplification was performed using 6 cycles of PCR for the 200 and 400 ng samples or 10 cycles for the 50 ng protocol. All tumour samples had matched buffy coat samples sequenced concurrently for variant calling to permit filtering of germline variants.

Sequencing

A clinically validated capture-based target enrichment gene panel was used (Supplementary Table 2). This panel was targeted to known cancer mutation hotspots, present in a wide array of solid tumours. Nimblegen Capture KAPA HyperPlus kits (Roche) were used for panel hybridisation. Quality control after hybridisation and PCR amplification were performed using TaqMan quantitative PCR prior to sample sequencing. Samples were sequenced on either a NextSeq or MiSeq platform (Illumina, San Diego, USA) according to manufacturer's user guides

Bioinformatics

Sequencing output files were demultiplexed using Bcl2fastq2 v.2.19 (Illumina) and aligned to reference genome GRCh37 using BWA-mem v.0.7.12 software. Data were filtered through an in-house pipeline that included GATK *Mutect2* version 3.5.0 (Broad Institute, Cambridge, Massachusetts) for single nucleotide variant (SNV) and insertion/deletion (Indel) annotation, and Manta v.0.29.6 for structural variants. Additional in-house filters applied to variant calling included deletion and amplification thresholds of <0.5x and >2.4x, respectively.

DNA extraction - Blood

20 mL of peripheral blood was collected from patients in cell-free DNA Blood Collection Tubes (Streck, La Vista, USA). Samples were centrifuged twice for 10 minutes at 1600g. Plasma was aliquoted and stored at -80°C. Cell-free DNA was extracted from approximately 4 mL of plasma using the QIAsymphony DSP Circulating DNA Kit (Qiagen, Hilden, Germany) on a QIAsymphony SP platform.

Plasma genotyping

Plasma samples were genotyped using the QX-200 droplet digital PCR system (Bio-Rad, California, USA). Custom Taqman assays were used (Bio-Rad & Applied Biosystems, Thermo Scientific) according to the variants discovered from tumour tissue sequencing. For each plasma time-point, 10.45 µL of DNA was placed per well in at least 2 wells and interrogated with the custom assays. Mean cfDNA concentration of samples was 0.43 ng/µL (range 0.079 – 1.47). For each patient-specific assay one No Template Control (NTC), one wild-type control (fragmented Promega DNA at 1 ng/µL) and one positive control (patient's own tumour DNA) were used. All custom assays detected their target variant in tumour controls with very high correlation (R^2 = 0.92) between NGS and dPCR tumour allele frequency (AF) (Supplementary Figure 1).

cfDNA samples were emulsified on a droplet generator. Emulsified PCR reactions were run on 96-well plates on a C1000 Touch Thermal Cycler (Bio-Rad), incubating the plates at 95°C for 10 min, followed by 40 cycles of 94°C for 30 s and 60°C for 60 s, then by a 10-min incubation at 98°C. The temperature ramp increment was 2.0°C/s for all steps. Samples were read on a QX-200 ddPCR droplet reader as per manufacturer's guidelines. Results were analysed using Bio-Rad's QuantaSoft software v.1.7.4, and individual cut-offs established for each assay. A minimum of 20,000 droplets across both wells was required for a valid test. A minimum of 2 single FAM positive droplets with a number of double positive droplets lower than single FAM droplets was required to make a positive call. If no positive result was obtained in 2 wells, then the assay was repeated for a further 2 wells.

Standard Biomarker Assays

The Access Thyroglobulin and Thyroglobulin Antibody II chemiluminescent immunoassays (Beckman Coulter, Brea, CA, USA) were used for Tg and anti-Tg antibody quantification, respectively. Calcitonin assay was done with the LIAISON® Calcitonin II-Gen one-step sandwich chemiluminescence immunoassay (DiaSorin, Saluggia, Italy). Quantitative CEA assaying was performed using the ARCHITECT chemiluminescent microparticle immunoassay (Abbott Laboratories, IL, USA).

Imaging

Contrast-enhanced CT scanning was used for axial imaging in this study, with views obtained of the head, neck, thorax, abdomen (liver imaging was initially triple phase at baseline, dual phase thereafter) and pelvis. Progression was defined as per RECIST criteria (22)

RESULTS

Tumour tissue mutational analysis

52 patients were recruited to the study (Figure 1). Tissue was not available for analysis in one patient. The histological subtypes of the final 51 patients were as follows: papillary (n = 17), follicular (15), medullary (15), poorly differentiated (3) and anaplastic (1). The clinical characteristics are summarised in Table 1 and shown in more detail in Supplementary Table 2. Tissue blocks were retrieved for DNA extraction in 50 cases. In one case, blocks were not available and DNA extraction was performed from H&E stained slides. We aimed to obtain a minimum of 3 plasma time-points, sampled every 3 months per patient where possible, and a mean of 5 time-points was achieved. A total of 190 plasma samples were assayed.

In total, 58 variants were discovered in 42 patients. At least one variant was detected in 82% of our patient cohort. All variants were either Single Nucleotide Variants (SNVs) or small insertion/deletions (Indels). A heatmap illustrating discovered variants is shown in Figure 2 (see supplementary table 3 for a full list of variants).

Histological sub-analysis of variants (**Figure 3**) showed that for PTC, the frequency of variants found in each mutated gene was broadly in line with rates previously published by the TCGA (23) as well as the mutated genes listed by the Catalogue of Somatic Mutations in Cancer (COSMIC) (24), as shown in figure 4a. All *BRAF* variants detected were the c.1799T>A (p.V600E) variant, which represented 13 of the 21 (61%) mutations discovered in the papillary subset. The most frequently mutated gene in the follicular cohort was NRAS, contributing 20% of the total variants, with similar rate to that seen in the COSMIC database (figure 4b). The mutation rates in genes obtained in our study compared to COSMIC for MTC are shown **Error! Reference source not found.**4c. The most commonly detected variant in the medullary cohort was *RET* c.2753T>C which accounted for 7 of 15 (46%) in concordance with other published data series (25). A *RET* mutation was entirely specific for a medullary histology in our cohort.

Nine patients had 2 or more driver mutations, and all these patients had metastatic disease. Histological subtypes associated with more aggressive disease, such as Hürthle cell and PDTC were over-represented in this group.

Plasma ctDNA detection

The primary end-point for the study was detection of plasma ctDNA, and in our cohort ctDNA was detected in at least one plasma time point in 67% (n=28/42) of patients. Based on histology, the detection rate was higher in MTC compared to PTC and FTC (Table 2). However, five patients had no identifiable macroscopic disease throughout the study, and negligible levels of conventional markers. If these patients were excluded from the analysis the detection rates were more balanced across the histologies and the overall detection rate increased to 76% (Table 2). The detection rate

was highest in patients with metastatic disease (79%) compared to those with local recurrence (33%) or no macroscopic disease (0%)

The secondary endpoint of the study was correlation of ctDNA with currently used biomarkers. In this cohort, a clear overall trend was observed where detected plasma ctDNA concentrations correlated with Tg, calcitonin and CEA. Statistical analysis revealed a significant positive correlation (r values >0.5) between concentrations of ctDNA and those of conventional biomarkers.

Scenarios where ctDNA may offer superiority over conventional biomarkers

Serial serum analysis demonstrated that ctDNA markers may provide clinically important advantages over current plasma biomarkers in a number of cases (Figures 5, 6 and 7). These include detection of ctDNA in the absence of other markers, earlier changes in ctDNA levels reflective of disease status and more rapid detection of change in disease status when the patient is started on targeted therapies.

Figure 5 shows ctDNA levels in two patients who had no usefully detectable levels of conventional biomarkers. One patient (Fig. 5a) had no Tg due to anti-Tg antibodies, and the other (Fig. 5b) had none as a result of severe tissue de-differentiation in anaplastic disease. Both patients had detectable ctDNA demonstrating upward trends before progression was detected with axial imaging.

In three patients with MTC who had evidence of progressive disease (clinically and on CT imaging) during surveillance, we observed earlier upward trends in ctDNA than the corresponding conventional biomarker (figures 6a-c). This could allow for earlier prediction of disease progression.

In several patients on targeted therapy for progressive disease, we observed changes in ctDNA titres that were more marked/rapid than conventional markers. This potentially allows for both earlier and more confident prediction of response to therapy (Figures 7a-d). Figures 7a-c illustrate more significant or earlier increases in ctDNA, likely reflecting development of resistance to the targeted therapy. Figure 7d demonstrates the reverse: an extremely large decrease in ctDNA levels is seen after starting effective TKI therapy. Conventional biomarkers were not able to track these changes so responsively.

In patients with 2 variants detected in the tumour which were tracked in the plasma, we observed significant differences in the levels of one variant compared to the other (Figures 5a, 7b, 7c). In one patient (Fig 7b), the *TP53* c.1009C>T variant was strongly positive in all samples, whereas the *TP53* c.742C>T variant was not detected in any plasma samples. In two other patients (Figs 5a & 7c), both variants are initially seen to monitor disease burden. However, the subsequent progression of disease is tracked by only one variant. Differential levels of alternative variants may provide insight into tumour evolution.

DISCUSSION

The aim of our study was to investigate the potential role of comprehensive multi-variant mutational analysis using next generation sequencing and to report findings that provide support for the use of plasma ctDNA as a biomarker in thyroid cancer. Examining multiple genes in a variety of thyroid cancer histologies, ctDNA was detected in 67% of patients in this study. Within the cohort of 42 patients in whom tumour variants were observed, 5 patients had no evidence of biochemical and structural disease throughout the study period. Therefore, the overall sensitivity for ctDNA detection was 76% (Table 2) and is comparable to rates obtained in other, more aggressive, cancers such as lung and breast (26).

Cote et al (20) recently evaluated the detection of a single variant, *RET* p.M918T, in the plasma of patients with MTC known to harbour this variant in their tumours. Their reported detection rate was only 32%. In our MTC cohort, the detection rate was much higher (85%, adjusted). Both the use of one genetic variant as a biomarker and a single time point analysis in the Cote study are likely to have been responsible for their lower detection rates. Interestingly, the rate of ctDNA detection was higher in patients with greater disease burden. This may also explain the higher detection rates for our study in MTC patients (79%, unadjusted) all of whom had metastatic disease compared to PTC patients (53%, unadjusted). Further, in the more aggressive histological sub-types (ATC and PDTC), ctDNA was always detected, although numbers were low.

The rates of variants detected in the tumour tissue for this study were broadly in line with published data and those of the TCGA and COSMIC databases. In the COSMIC database, the gene most frequently observed to have variants in FTC is *TERT*. Our targeted gene panel did not include this gene, so *TERT* mutations were not detectable in our study.

Analysis of serial serum samples demonstrated a clear trend where detected plasma ctDNA concentrations correlated with conventional biomarkers; Tg, calcitonin and CEA levels, and with disease status (disease response/progression) defined by axial imaging. Although the current study was primarily designed to evaluate ctDNA as a potential biomarker in thyroid cancer, our data provide early indications that ctDNA represents an important complementary assay and could offer several advantages over conventional markers.

ctDNA may prove to be an important biomarker of disease burden and response to treatment in patients when thyroglobulin cannot be used for monitoring, such as in patients with significant anti-thyroglobulin antibodies, and in de-differentiated thyroid cancers. In our study, one patient had undetectable thyroglobulin and significant anti-thyroglobulin antibodies at all time-points, yet ctDNA was detected for two variants in this patient's plasma and exhibited an upward trend in the *BRAF* variant coinciding with disease progression later confirmed on subsequent axial imaging (figure 5a). In a further patient with anaplastic carcinoma, the conventional biomarker (Tg) was not detectable, presumably due to tumour de-differentiation (figure 5b). However, ctDNA was detectable at all time points and exhibited an upward trend consistent with disease progression which was later confirmed on axial imaging, and the patient subsequently died from the disease. Therefore, ctDNA may represent an important biomarker in anaplastic and de-differentiated thyroid cancers, particularly if effective therapies become available in the future.

In this study, ctDNA levels appear to change more rapidly in response to a change in disease status than conventional markers and may offer a more contemporaneous measure of response to treatment. In multiple patients, we observed an upward trend in ctDNA earlier (4-8 months earlier) than the corresponding conventional biomarker (figure 6), or a significantly more marked increase in levels (figure 7a-c), allowing not only for earlier but also more confident prediction of disease progression. These trends were later confirmed by axial imaging demonstrating disease progression.

Assessing early biological response to targeted therapy and ascertaining when resistance develops in patients with thyroid cancer has traditionally been difficult, and ctDNA could potentially assist in this setting. In several patients, we detected marked and rapid reduction of ctDNA levels (figures 5a, 7c, 7d) shortly after starting systemic targeted therapy. The more rapid responses of ctDNA levels in response to targeted therapy seen in this study would be useful in gauging early response to treatment. On the other hand, this might be show greatest clinical value in detecting futility of therapy, thereby allowing prompt cessation of a potentially toxic but ineffective treatment. Further, development of resistance to treatment appears to be detected by ctDNA rises after the initial drop. It is evident that such changes in response cannot always to be monitored by conventional biomarkers (Figs 5a, 6b, 7b-d). Prompt detection of resistance would allow the timely addition of alternative therapeutic agents to overcome newly-developing resistance. These more rapid changes in ctDNA concentrations may reflect significant differences in biomarker half-lives, which may be as low as 2 hours in ctDNA (13) and up to 65 hours for thyroglobulin (27, 28).

Much has been published on the dynamic mutational landscape of cancers as a result of subclonal evolution (10-12), but data are sparse in thyroid cancer. In 3 patients, there was a substantial difference between the trends in the two tracked variants in the ctDNA, which was not reflective of the differences in tumour allele frequencies seen in the NGS results. This discrepancy may reflect subclonal evolution, as the tumour tissue samples often pre-dated the plasma samples by many years (Supplementary table 1). Discordant results obtained in the plasma may reflect one subclone emerging as more dominant than another. This has implications for patient therapy: knowledge of a dominant subclone may influence choice of intervention.

With the latest assays permitting consistent interpretation of sequencing at much higher read depth from significantly lower allele fractions, it is now feasible to sequence DNA extracted directly from plasma samples. We aim to apply this approach over serial plasma samples in thyroid cancer subtypes in order to track the changing mutational landscape without the need for repeated tissue biopsies. This may help overcome difficulties related to intra-tumour heterogeneity that is inherent in tissue biopsies. Further, several studies have demonstrated that ctDNA can be used to detect resistance-conferring mutations in both breast and lung cancer (29-31) and, although resistance mutations are not currently known in thyroid cancer, our study data suggest this is a feasible direction of study and warrants further investigation.

CONCLUSION

This study demonstrates that, using a multi-variant approach, a high proportion of patients with advanced thyroid cancer have detectable levels of ctDNA in their plasma. We observed correlation of ctDNA with conventional markers of disease in DTC. We suggest, based on our data, that ctDNA may be particularly useful when conventional markers are not helpful, for example in de-differentiated disease or when anti-Tg antibodies render Tg an unreliable marker. ctDNA is, therefore, likely to complement current conventional biomarkers in the management of thyroid cancer. Further, our data suggest that ctDNA may predict disease progression earlier and more confidently than conventional markers, particularly in MTC. For patients on targeted therapies, ctDNA may offer a more rapid and reliable assessment of disease response, providing information on effectiveness of therapies and guiding drug selection. These early results are promising and ctDNA may prove to be a clinically useful biomarker in thyroid cancer. Further investigation with a larger sample size is required to confirm these initial findings.

FIGURES AND TABLES

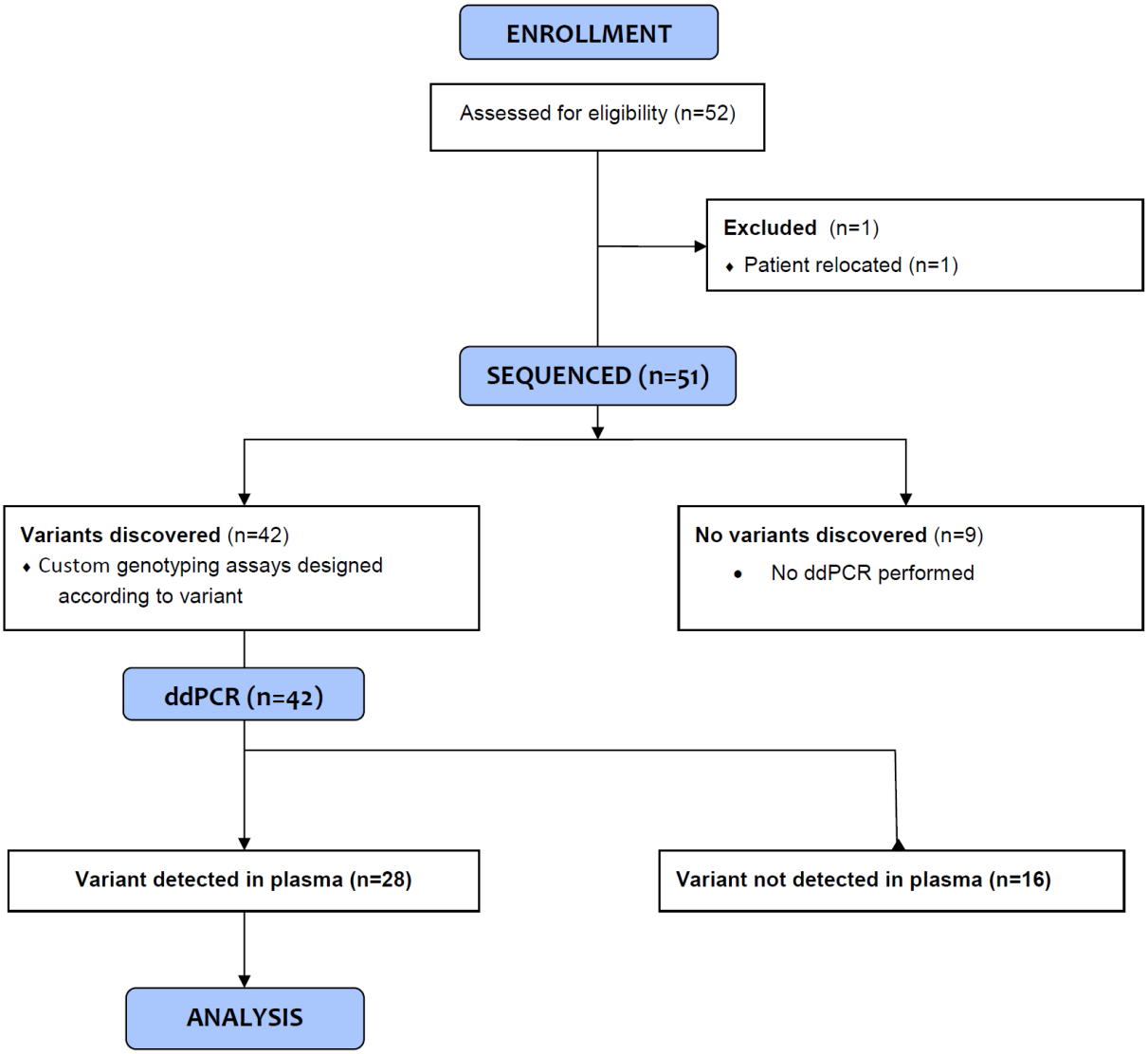

Figure 1 – CONSORT diagram of study

Clinical Characteristics

Demographics	
Median Age, years (Range)	*61 (27 – 81)*
Female, n (%)	*26 (51)*
Tumour Histology	
Papillary, n (%)	*17 (34)*
Follicular	*15 (29)*
Poorly Differentiated	*3 (6)*
Anaplastic	*1 (2)*
Medullary	*15 (29)*
Disease Status at study entry	
No structural disease, n (%)	*6 (12)*
Local recurrence	*2 (4)*
Distant metastasis	*43 (84)*

Table 1 – Summary of patient clinical characteristics

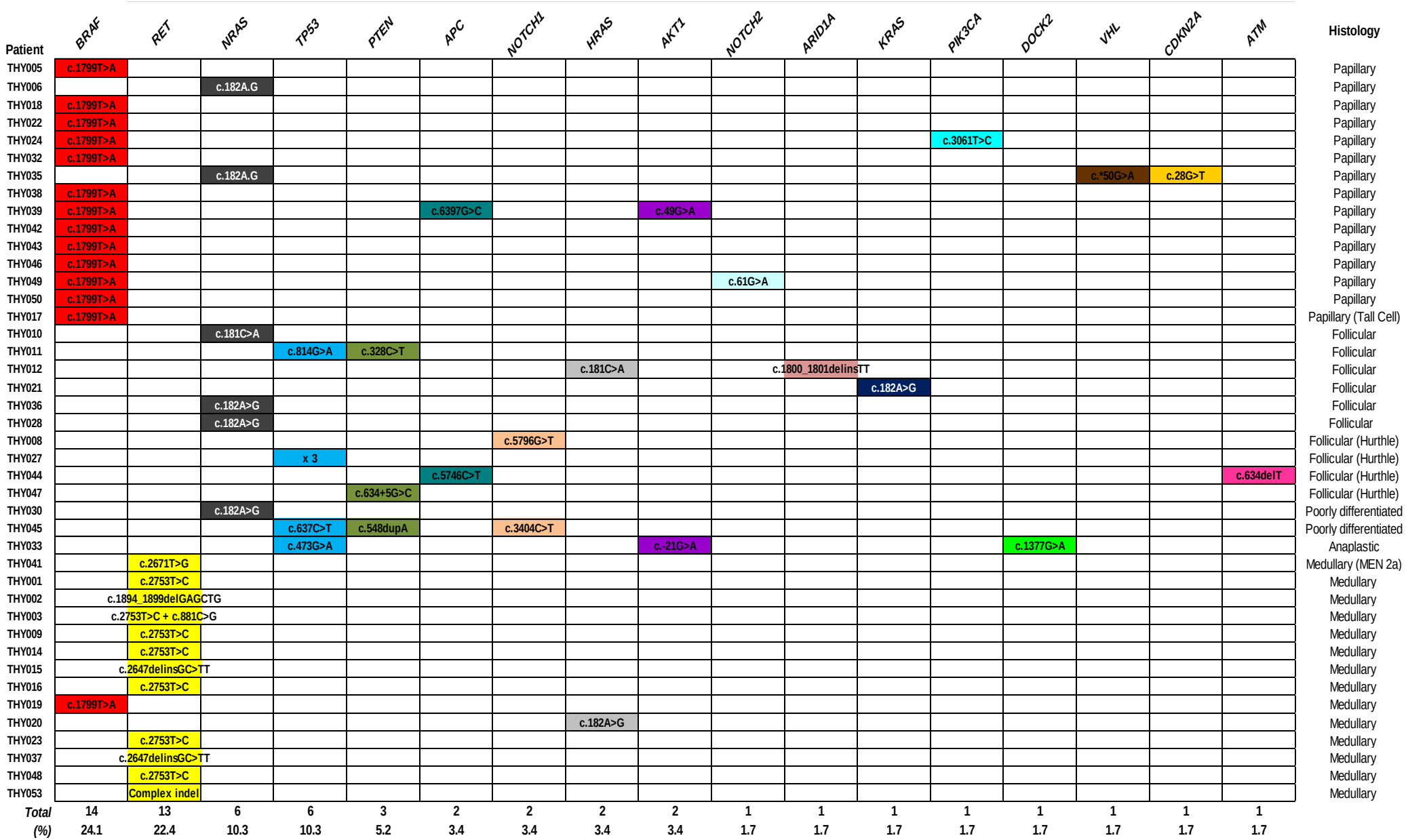

Patient	BRAF	RET	NRAS	TP53	PTEN	APC	NOTCH1	HRAS	AKT1	NOTCH2	ARID1A	KRAS	PIK3CA	DOCK2	VHL	CDKN2A	ATM	Histology
THY005	c.1799T>A																	Papillary
THY006			c.182A.G															Papillary
THY018	c.1799T>A																	Papillary
THY022	c.1799T>A																	Papillary
THY024	c.1799T>A												c.3061T>C					Papillary
THY032	c.1799T>A																	Papillary
THY035			c.182A.G												c.*50G>A	c.28G>T		Papillary
THY038	c.1799T>A																	Papillary
THY039	c.1799T>A					c.6397G>C			c.49G>A									Papillary
THY042	c.1799T>A																	Papillary
THY043	c.1799T>A																	Papillary
THY046	c.1799T>A																	Papillary
THY049	c.1799T>A									c.61G>A								Papillary
THY050	c.1799T>A																	Papillary
THY017	c.1799T>A																	Papillary (Tall Cell)
THY010			c.181C>A															Follicular
THY011				c.814G>A	c.328C>T													Follicular
THY012								c.181C>A			c.1800_1801delinsTT							Follicular
THY021												c.182A>G						Follicular
THY036			c.182A>G															Follicular
THY028			c.182A>G															Follicular
THY008							c.5796G>T											Follicular (Hurthle)
THY027				x 3														Follicular (Hurthle)
THY044						c.5746C>T											c.634delT	Follicular (Hurthle)
THY047					c.634+5G>C													Follicular (Hurthle)
THY030			c.182A>G															Poorly differentiated
THY045				c.637C>T	c.548dupA		c.3404C>T											Poorly differentiated
THY033				c.473G>A					c.-21G>A					c.1377G>A				Anaplastic
THY041		c.2671T>G																Medullary (MEN 2a)
THY001		c.2753T>C																Medullary
THY002	c.1894_1899delGAGCTG																	Medullary
THY003	c.2753T>C + c.881C>G																	Medullary
THY009		c.2753T>C																Medullary
THY014		c.2753T>C																Medullary
THY015	c.2647delinsGC>TT																	Medullary
THY016		c.2753T>C																Medullary
THY019	c.1799T>A																	Medullary
THY020								c.182A>G										Medullary
THY023		c.2753T>C																Medullary
THY037	c.2647delinsGC>TT																	Medullary
THY048		c.2753T>C																Medullary
THY053		Complex indel																Medullary
Total	14	13	6	6	3	2	2	2	2	1	1	1	1	1	1	1	1	
(%)	24.1	22.4	10.3	10.3	5.2	3.4	3.4	3.4	3.4	1.7	1.7	1.7	1.7	1.7	1.7	1.7	1.7	

Figure 2 - Mutation heat map from study cohort

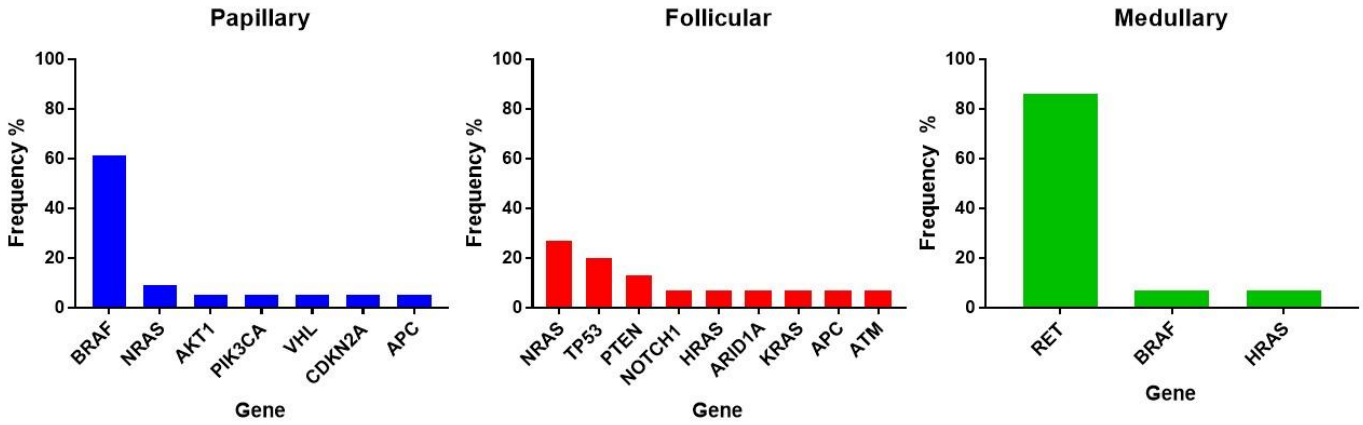

Figure 3 *–frequency of variants found in each cancer subtype per gene*

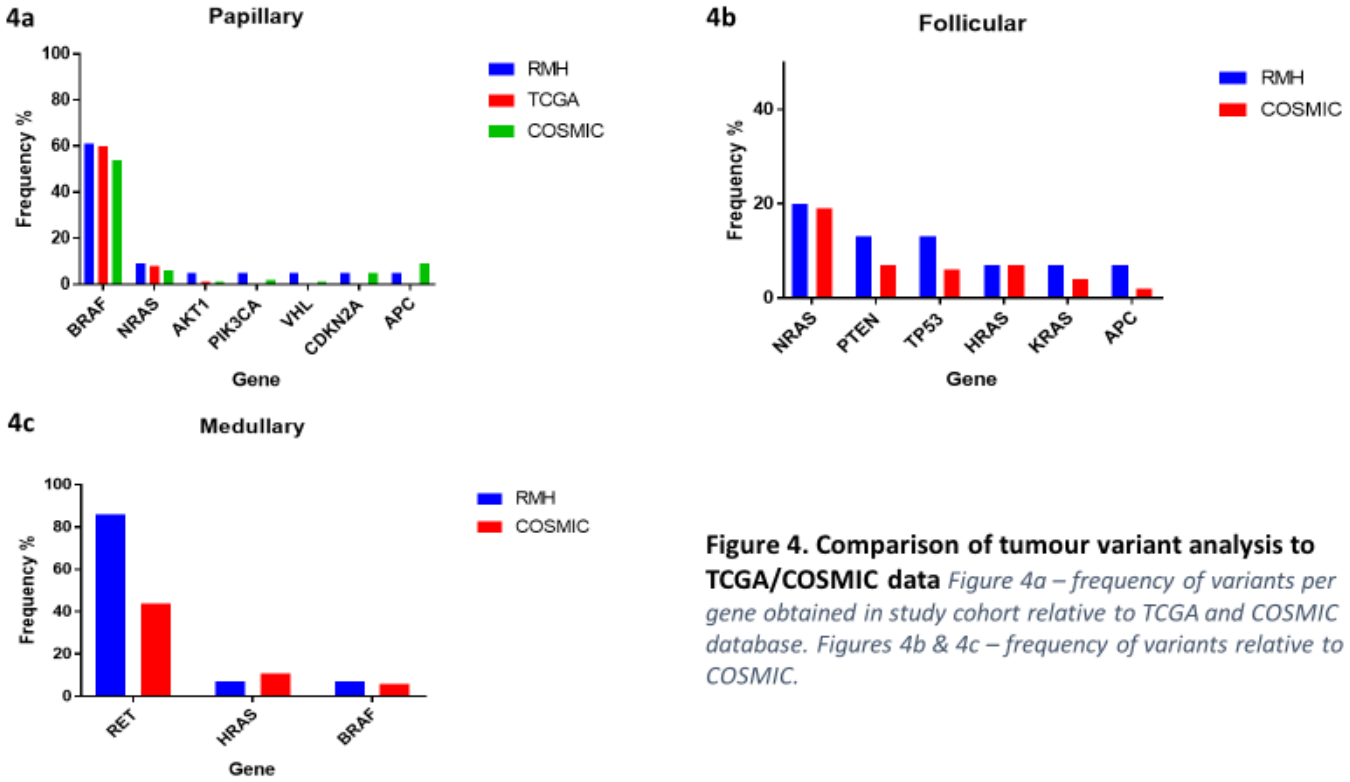

Figure 4. Comparison of tumour variant analysis to TCGA/COSMIC data *Figure 4a – frequency of variants per gene obtained in study cohort relative to TCGA and COSMIC database. Figures 4b & 4c – frequency of variants relative to COSMIC.*

Histology *(n)*	Detection Rate	*Adjusted*
Papillary *(15)*	53%	*73%*
Follicular *(10)*	60%	*60%*
Medullary *(14)*	79%	*85%*
PDTC *(2)*	100%	*100%*
ATC *(1)*	100%	*100%*
Total (42)	**67%**	***76%***

*Table 2 – **Detection rate:** detection rates in patients of ctDNA in at least one plasma time point. **Adjusted:** detection rates adjusted for 5 patients with no macroscopic disease and negligible conventional markers*

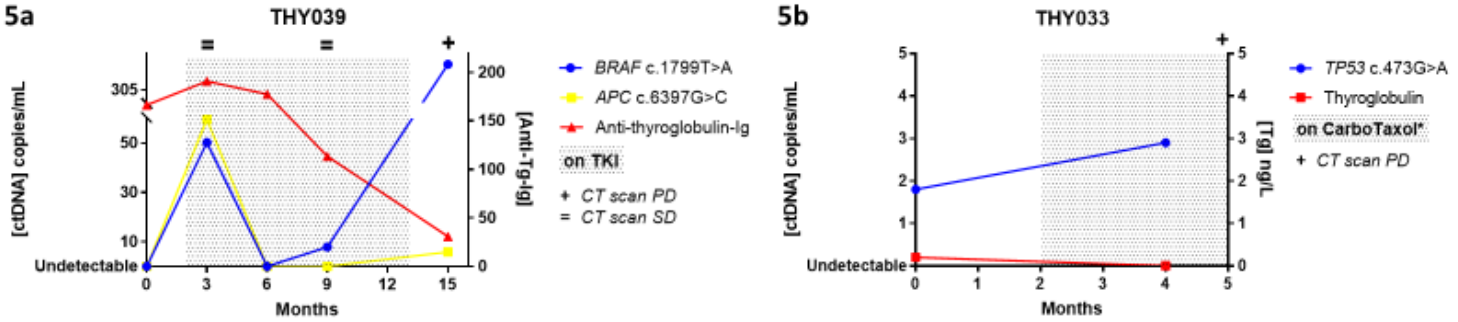

Figure 5. Detection of ctDNA when conventional markers absent.

***Figure 5a** – Patient with papillary carcinoma and undetectable Tg levels due to Anti-Tg-Ig. Two ctDNA variants are detectable in the plasma. A drop in ctDNA levels can be seen at month 6 which likely reflexcts an initial response of the disease to commencing TKI therapy (Sorafenib). This is followed by an increase in the BRAF variant prior to disease progression from month 9 onwards. Progression was later confirmed on axial imaging. The second variant in APC remains low, and is presumed to reflect a non-dominant subclone. Anti-Tg-Ig is seen to be trending downwards despite proven progressive disease. **Figure 5b** – Patient with anaplastic carcinoma and negligible/undetectable Tg levels due to advanced tissue de-dedifferentiation. ctDNA levels are seen to increase prior to disease progression, confirmed at month 5 with axial imaging. The patient subsequently died of the disease.*

**CarboTaxol: chemotherapy regimen of Paclitaxel and Carboplatin. CT Scan PD: Progressive Disease detected on CT axial imaging as per RECIST criteria. CT Scan SD: Stable disease. Shaded area represents period patient was on therapy.*

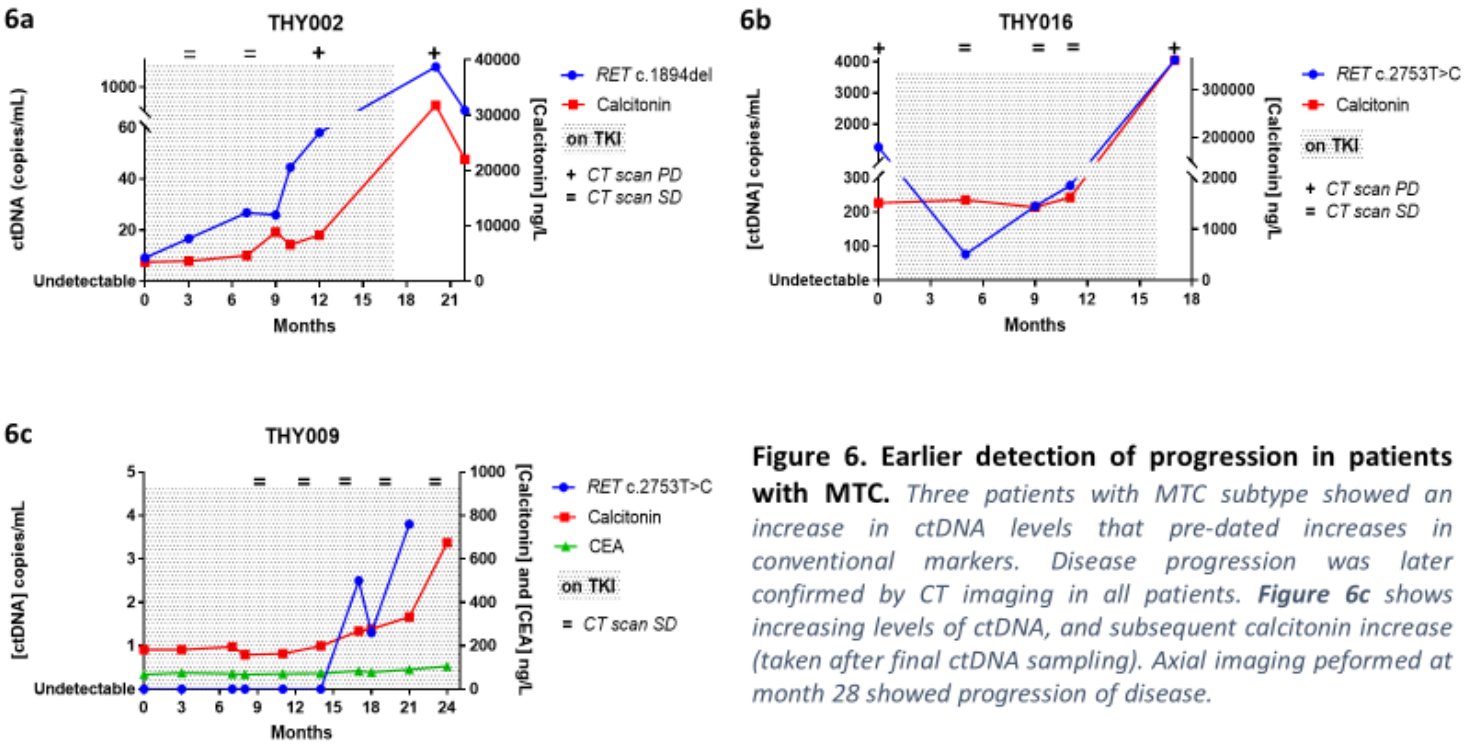

Figure 6. Earlier detection of progression in patients with MTC. *Three patients with MTC subtype showed an increase in ctDNA levels that pre-dated increases in conventional markers. Disease progression was later confirmed by CT imaging in all patients. **Figure 6c** shows increasing levels of ctDNA, and subsequent calcitonin increase (taken after final ctDNA sampling). Axial imaging peformed at month 28 showed progression of disease.*

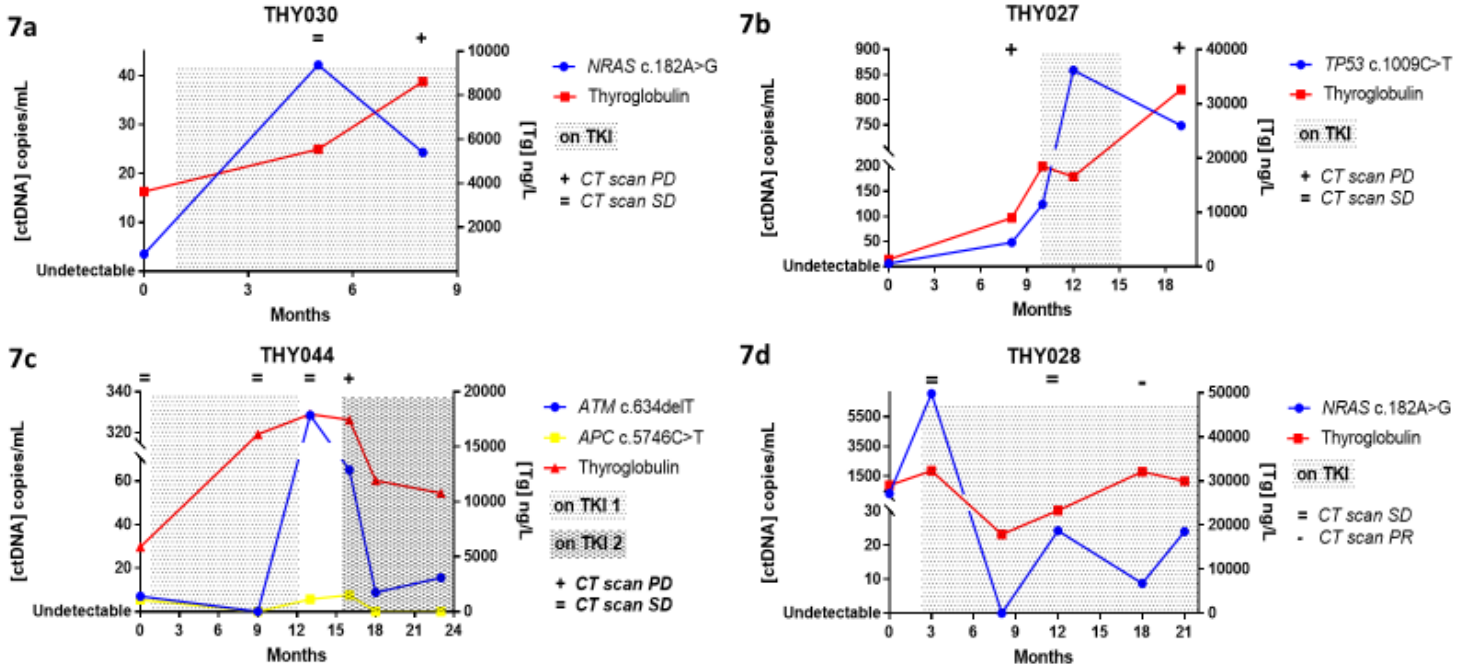

Figure 7. More responsive changes in ctDNA levels reflective of disease status ***Figure 7a –*** *Ten-fold increase in ctDNA prior to CT progession. A similar increase is not seen in Tg levels, potentially offering more confident prediction of non-response to TKI.* ***Figure 7b*** *– Significant increase in plasma ctDNA levels at month 12, indicating non-response to TKI, not mirrored in Tg until later.* ***Figure 7c –*** *Larger scale changes in ctDNA relative to Tg at month 12 and month 18 indicating disease progression followed by likely response to TKI.* ***Figure 7d –*** *marked ctDNA drop observed at month 8 following commencement of TKI, indicating disease response, confirmed later by axial imaging.*

REFERENCES

1. Pacini F, Mariotti S, Formica N, Elisei R, Anelli S, Capotorti E, et al. Thyroid autoantibodies in thyroid cancer: incidence and relationship with tumour outcome. Acta endocrinologica. 1988;119(3):373-80.
2. Spencer CA, Takeuchi M, Kazarosyan M, Wang CC, Guttler RB, Singer PA, et al. Serum thyroglobulin autoantibodies: prevalence, influence on serum thyroglobulin measurement, and prognostic significance in patients with differentiated thyroid carcinoma. The Journal of clinical endocrinology and metabolism. 1998;83(4):1121-7.
3. Garcia-Murillas I, Schiavon G, Weigelt B, Ng C, Hrebien S, Cutts RJ, et al. Mutation tracking in circulating tumor DNA predicts relapse in early breast cancer. Science translational medicine. 2015;7(302):302ra133.
4. Lee RJ, Gremel G, Marshall A, Myers KA, Fisher N, Dunn J, et al. Circulating tumor DNA predicts survival in patients with resected high risk stage II/III melanoma. Annals of oncology : official journal of the European Society for Medical Oncology. 2017.
5. Reinert T, Scholer LV, Thomsen R, Tobiasen H, Vang S, Nordentoft I, et al. Analysis of circulating tumour DNA to monitor disease burden following colorectal cancer surgery. Gut. 2016;65(4):625-34.
6. U.S. Food and Drug Administration: Medical Devices: cobas EGFR Mutation Test v2 - P150047: U.S. Food and Drug Administration; 2016 [updated 02/04/2018. Available from: https://www.accessdata.fda.gov/scripts/cdrh/cfdocs/cfpma/pma.cfm?id=P150047.
7. Stroun M, Lyautey J, Lederrey C, Olson-Sand A, Anker P. About the possible origin and mechanism of circulating DNA apoptosis and active DNA release. Clinica chimica acta; international journal of clinical chemistry. 2001;313(1-2):139-42.
8. Jahr S, Hentze H, Englisch S, Hardt D, Fackelmayer FO, Hesch RD, et al. DNA fragments in the blood plasma of cancer patients: quantitations and evidence for their origin from apoptotic and necrotic cells. Cancer research. 2001;61(4):1659-65.
9. Diaz LA, Jr., Bardelli A. Liquid biopsies: genotyping circulating tumor DNA. Journal of clinical oncology : official journal of the American Society of Clinical Oncology. 2014;32(6):579-86.
10. Gerlinger M, Rowan AJ, Horswell S, Larkin J, Endesfelder D, Gronroos E, et al. Intratumor heterogeneity and branched evolution revealed by multiregion sequencing. The New England journal of medicine. 2012;366(10):883-92.
11. Jamal-Hanjani M, Wilson GA, McGranahan N, Birkbak NJ, Watkins TBK, Veeriah S, et al. Tracking the Evolution of Non-Small-Cell Lung Cancer. The New England journal of medicine. 2017.
12. Abbosh C, Birkbak NJ, Wilson GA, Jamal-Hanjani M, Constantin T, Salari R, et al. Phylogenetic ctDNA analysis depicts early-stage lung cancer evolution. Nature. 2017;545(7655):446-51.
13. Diehl F, Schmidt K, Choti MA, Romans K, Goodman S, Li M, et al. Circulating mutant DNA to assess tumor dynamics. Nat Med. 2008;14(9):985-90.
14. Tie J, Wang Y, Tomasetti C, Li L, Springer S, Kinde I, et al. Circulating tumor DNA analysis detects minimal residual disease and predicts recurrence in patients with stage II colon cancer. Science translational medicine. 2016;8(346):346ra92.
15. Chaudhuri AA, Chabon JJ, Lovejoy AF, Newman AM, Stehr H, Azad TD, et al. Early Detection of Molecular Residual Disease in Localized Lung Cancer by Circulating Tumor DNA Profiling. Cancer discovery. 2017.
16. Abbosh C, Birkbak NJ, Wilson GA, Jamal-Hanjani M, Constantin T, Salari R, et al. Phylogenetic ctDNA analysis depicts early stage lung cancer evolution. Nature. 2017.
17. Chuang TC, Chuang AY, Poeta L, Koch WM, Califano JA, Tufano RP. Detectable BRAF mutation in serum DNA samples from patients with papillary thyroid carcinomas. Head & neck. 2010;32(2):229-34.
18. Cradic KW, Milosevic D, Rosenberg AM, Erickson LA, McIver B, Grebe SK. Mutant BRAF(T1799A) can be detected in the blood of papillary thyroid carcinoma patients and correlates with disease status. The Journal of clinical endocrinology and metabolism. 2009;94(12):5001-9.
19. Pupilli C, Pinzani P, Salvianti F, Fibbi B, Rossi M, Petrone L, et al. Circulating BRAFV600E in the diagnosis and follow-up of differentiated papillary thyroid carcinoma. The Journal of clinical endocrinology and metabolism. 2013;98(8):3359-65.

20. Cote GJ, Evers C, Hu MI, Grubbs EG, Williams MD, Hai T, et al. Prognostic Significance of Circulating RET M918T Mutated Tumor DNA in Patients With Advanced Medullary Thyroid Carcinoma. The Journal of clinical endocrinology and metabolism. 2017;102(9):3591-9.
21. Sandulache VC, Williams MD, Lai SY, Lu C, William WN, Busaidy NL, et al. Real-Time Genomic Characterization Utilizing Circulating Cell-Free DNA in Patients with Anaplastic Thyroid Carcinoma. Thyroid : official journal of the American Thyroid Association. 2017;27(1):81-7.
22. Eisenhauer EA, Therasse P, Bogaerts J, Schwartz LH, Sargent D, Ford R, et al. New response evaluation criteria in solid tumours: revised RECIST guideline (version 1.1). European journal of cancer (Oxford, England : 1990). 2009;45(2):228-47.
23. Cancer Genome Atlas Research N. Integrated genomic characterization of papillary thyroid carcinoma. Cell. 2014;159(3):676-90.
24. Forbes SA, Beare D, Boutselakis H, Bamford S, Bindal N, Tate J, et al. COSMIC: somatic cancer genetics at high-resolution. Nucleic Acids Research. 2017;45(D1):D777-D83.
25. Ji JH, Oh YL, Hong M, Yun JW, Lee HW, Kim D, et al. Identification of Driving ALK Fusion Genes and Genomic Landscape of Medullary Thyroid Cancer. PLoS genetics. 2015;11(8):e1005467.
26. Bettegowda C, Sausen M, Leary RJ, Kinde I, Wang Y, Agrawal N, et al. Detection of circulating tumor DNA in early- and late-stage human malignancies. Science translational medicine. 2014;6(224):224ra24.
27. Hocevar M, Auersperg M, Stanovnik L. The dynamics of serum thyroglobulin elimination from the body after thyroid surgery. European journal of surgical oncology : the journal of the European Society of Surgical Oncology and the British Association of Surgical Oncology. 1997;23(3):208-10.
28. Giovanella L, Ceriani L, Maffioli M. Postsurgery serum thyroglobulin disappearance kinetic in patients with differentiated thyroid carcinoma. Head & neck. 2010;32(5):568-71.
29. Sefrioui D, Perdrix A, Sarafan-Vasseur N, Dolfus C, Dujon A, Picquenot J-M, et al. Short report: Monitoring ESR1 mutations by circulating tumor DNA in aromatase inhibitor resistant metastatic breast cancer. International journal of cancer. 2015;137(10):2513-9.
30. Thompson JC, Yee SS, Troxel AB, Savitch SL, Fan R, Balli D, et al. Detection of therapeutically targetable driver and resistance mutations in lung cancer patients by next generation sequencing of cell-free circulating tumor DNA. Clinical cancer research : an official journal of the American Association for Cancer Research. 2016;22(23):5772-82.
31. Taniguchi K, Uchida J, Nishino K, Kumagai T, Okuyama T, Okami J, et al. Quantitative Detection of EGFR Mutations in Circulating Tumor DNA Derived from Lung Adenocarcinomas. Clinical Cancer Research. 2011;17(24):7808-15.

SUPPLEMENTARY MATERIALS

Trial ID	Sex	Age at study entry	TNM Staging at diagnosis	Tumour Histology	Disease Status at study entry	Location of metastasis, if present	Time: diagnosis to study entry (years)
THY005	F	62	T3 N0 M1	Papillary	Distant Met	Mediastinum, Lung	8
THY006	F	74	T4a Nx M1	Papillary	Distant Met	Lung, Mediastinum, Bone	15
THY018	F	61	T3 N0 M0	Papillary	No Macroscopic Disease		1
THY022	F	64	T2 Nx M0	Papillary	Distant Met	Brain, Lung, Spine, Humerus	14
THY024	M	69	T4 N1 M0	Papillary	Distant Met	Thyroid Bed, Mediastinum, Pulmonary	12
THY032	F	46	T3 N1b M0	Papillary	Distant Met	Lung	5
THY035	M	74	T3 N1b M0	Papillary	Distant Met	Lung, Bone, Adrenal, Mediastinal, Local	2
THY038	F	47	T3 N0 M0	Papillary	No Macroscopic Disease		1
THY039	F	71	T4b N0 M0	Papillary	Distant Met	Bone, Chest wall, Local nodal	18
THY042	M	58	T2 N0 M0	Papillary	Distant Met	Lung, Local Nodal	13
THY043	F	66	T1 N0 M0	Papillary	Distant Met	Lung, Mediastinum	6
THY046	F	57	T3 N1b M0	Papillary	No Macroscopic Disease		3
THY049	M	56	T3 N1b M0	Papillary	Local recurrence		1
THY050	M	27	T3 N1b M0	Papillary	No Macroscopic Disease		6
THY051	M	60	T3 Nx M0	Papillary	Distant Met	Mediastinum, Supraclavicular Fossa	9
THY007	M	48	T3 N0 M0	Papillary (Tall Cell)	Distant Met	Brain	6
THY017	M	46	T4a N1b M1	Papillary (Tall Cell)	Distant Met	Lung, Spine	5
THY010	F	77	T3 Nx M0	Follicular	Distant Met	Lung	11
THY011	F	30	T3 N0 M0	Follicular	Distant Met	Lung, Brain, Bone, Nodal	3
THY012	M	72	T3 N0 M1	Follicular	Distant Met	Bone	8
THY021	F	78	T3 N0 M0	Follicular	Local recurrence		1
THY034	M	64	T2 N0 M0	Follicular	Distant Met	Lung	3
THY036	M	56	T2 N1b M0	Follicular	Distant Met	Lung	5
THY040	M	73	T1b Nx M1	Follicular	Distant Met	Bone	1
THY028	F	61	T1b N0 M1	Follicular	Distant Met	Lung, Bone	5
THY008	F	67	T2 Nx M0	Follicular (Hurthle)	Distant Met	Liver, Lung	6
THY013	F	81	T1b N0 M0	Follicular (Hurthle)	Distant Met	Thyroid Bed, Lung	21
THY026	M	74	T4 N0 M0	Follicular (Hurthle)	Distant Met	Lung, Renal, Mediastinal	9
THY027	M	51	T3 N1b M1	Follicular (Hurthle)	Distant Met	Lung	3
THY029	F	48	Tx Nx M1	Follicular (Hurthle)	Distant Met	Mediastinum, Spine, Lung	8
THY044	F	49	T3 N1a M1	Follicular (Hurthle)	Distant Met	Mediastinum, Liver, Bone	5
THY047	M	73	T3 N0 M0	Follicular (Hurthle)	Distant Met	Bone (rib)	5
THY031	F	70	T3 N0 M0	Poorly differentiated	Distant Met	Lung	4
THY045	F	67	T3 N1a M1	Poorly differentiated	Distant Met	Lung, Mediastinum	1
THY030	F	63	T2 N0 M0	Poorly differentiated	Distant Met	Liver, Brain, Local	9
THY033	M	66	T4b Nx M0	Anaplastic	Distant Met	Bone, Local, Mediastinum, Lung	1
THY001	M	54	T3 N1b M1	Medullary	Distant Met	Lung, Liver, Mediastinum	1
THY020	F	67	T2 N1b M0	Medullary	Distant Met	Spine	16
THY023	F	33	T3 N1b M1	Medullary	Distant Met	Liver, Mediastinum, Local nodal	1
THY053	F	75	T2 N1b M0	Medullary	No Macroscopic Disease		11
THY002	M	45	T4a N1b M1	Medullary	Distant Met	Liver	2
THY003	F	71	Tx N1a M0	Medullary	Local recurrence		3
THY009	M	59	T4a N1b M0	Medullary	Distant Met	Supraclavicular fossa	7
THY014	M	68	Tx Nx M0	Medullary	Distant Met	Mediastinal, pericardial	33
THY015	M	41	Tx N1b M1	Medullary	Distant Met	Lung, Liver, Brain	11
THY016	M	54	T2 N1a M1	Medullary	Distant Met	Liver, Spine, Lung, Local	14
THY019	M	28	T3 N1b M1	Medullary	Distant Met	Mediastinal, Liver, Bone	4
THY037	M	67	T2 N1b N0	Medullary	Distant Met	Bone, Liver, Lung, Mediastinal	29
THY048	F	30	Tx N1b M1	Medullary	Distant Met	Local Nodal, Lung, Bone, Breast, Liver, Mediastinum	<1
THY041	M	32	T4a N1a M0	Medullary (MEN 2a)	Distant Met	Bone, Orbit, Tracheal	15
THY025	F	39	TxNxMx	Medullary (MEN 2a)	Distant Met	Liver, Lung, Oesophageal, Spine	13

Supplementary table 1 – Clinical characteristics of enrolled patients

Gene
AKT1
APC
ARID1A
ATM
BRAF
ARID1A
ATM
CDKN2A
CDKN2B
CTNNB1
DOCK2
EGFR
ELMO1
ERBB2
ERBB4
FBXW7
HRAS
IDH1
IDH2
JAK3
KIT
KRAS
MAP2K1
MAP2K2
NOTCH 1
NOTCH2
NOTCH3
NRAS
PDGFRA
PIK3CA
PTEN
RET
ROS1
SMAD4
TCF7L2
TP53
UGT1A1
VHL

Supplementary Table 2 - List of Genes in Targeted Panel

Trial ID	GENE	PROTEIN	HGVS	TAF
THY033	*AKT1*	n/a	c.-21G>A	0.31
THY039	*AKT1*	p.Glu17Lys	c.49G>A	0.29
THY039	*APC*	p.Asp2133His	c.6397G>C	0.32
THY044	*APC*	p.Gln1916Ter	c.5746C>T	0.39
THY012	*ARID1A*	p.Gln601Ter	c.1800GC>TT	0.34
THY044	*ATM*	p.Phe213fs	c.634delT	0.71
THY005	*BRAF*	p.Val600Glu	c.1799T>A	Man
THY017	*BRAF*	p.Val600Glu	c.1799T>A	0.49
THY018	*BRAF*	p.Val600Glu	c.1799T>A	0.22
THY019	*BRAF*	p.Val600Glu	c.1799T>A	0.43
THY022	*BRAF*	p.Val600Glu	c.1799T>A	Man
THY024	*BRAF*	p.Val600Glu	c.1799T>A	0.07
THY032	*BRAF*	p.Val600Glu	c.1799T>A	0.31
THY038	*BRAF*	p.Val600Glu	c.1799T>A	0.36
THY039	*BRAF*	p.Val600Glu	c.1799T>A	0.38
THY042	*BRAF*	p.Val600Glu	c.1799T>A	0.4
THY043	*BRAF*	p.Val600Glu	c.1799T>A	Man
THY046	*BRAF*	p.Val600Glu	c.1799T>A	0.23
THY049	*BRAF*	p.Val600Glu	c.1799T>A	0.16
THY050	*BRAF*	p.Val600Glu	c.1799T>A	0.37
THY035	*CDKN2A*	p.Glu10Ter	c.28G>T	0.08
THY033	*DOCK2*	p.T459T	c.1377G>A	0.29
THY012	*HRAS*	p.Gln61Lys	c.181C>A	0.76
THY020	*HRAS*	p.Gln61Arg	c.182A>G	0.41
THY021	*KRAS*	p.Gln61Arg	c.182A>G	0.39
THY008	*NOTCH1*	p.Leu1932Phe	c.5796G>T	0.07
THY045	*NOTCH1*	p.Ala1135Val	c.3404C>T	0.37
THY049	*NOTCH2*	p.Ala21Thr	c.61G>A	0.12
THY006	*NRAS*	p.Gln61Arg	c.182A>G	0.45
THY010	*NRAS*	p.Gln61Lys	c.181C>A	0.49
THY028	*NRAS*	p.Gln61Arg	c.182A>G	0.54
THY030	*NRAS*	p.Gln61Arg	c.182A>G	0.48
THY035	*NRAS*	p.Gln61Arg	c.182A>G	0.43
THY036	*NRAS*	p.Gln61Arg	c.182A>G	0.39
THY024	*PIK3CA*	p.Tyr1021His	c.3061T>C	0.09
THY011	*PTEN*	p.Gln110Ter	c.328C>T	0.75
THY045	*PTEN*	p.Asn184fs	c.548dupA	0.64
THY047	*PTEN*	n/a	c.634+5G>C	0.62
THY001	*RET*	p.Met918Thr	c.2753T>C	0.45
THY002	*RET*	p.Glu632_Leu633del	c.1894_1899delGAGCTG	0.33
THY003	*RET*	p.Ala294Gly	c.881C>G	0.18
THY003	*RET*	p.Met918Thr	c.2753T>C	0.18
THY009	*RET*	p.Met918Thr	c.2753T>C	0.36
THY014	*RET*	p.Met918Thr	c.2753T>C	0.44
THY015	*RET*	p.Ala883Ser	c.2647GG>TT	0.24
THY016	*RET*	p.Met918Thr	c.2753T>C	0.48
THY023	*RET*	p.Met918Thr	c.2753T>C	0.39

THY037	*RET*	p.Ala883Ser	c.2647GC>TT	0.28
THY041	*RET*	p.Ser891Ala	c.2671T>G	0.21
THY048	*RET*	p.Met918Thr	c.2753T>C	0.67
THY053	*RET*		complex indel	0.4
THY011	*TP53*	p.Val272Met	c.814G>A	0.65
THY027	*TP53*	p.Arg337Cys	c.1009C>T	0.29
THY027	*TP53*	p.Asp281His	c.841G>C	0.06
THY027	*TP53*	p.Arg248Trp	c.742C>T	0.15
THY033	*TP53*	p.Arg158His	c.473G>A	0.28
THY045	*TP53*	p.Arg213Ter	c.637C>T	0.63
THY035	*VHL*	n/a	c.*50G>A	0.12

Supplementary Table 3 – List of detected variants from NGS. TAF: tumour allele frequency, HGVS: Human Genome Variation Society annotation. Man: low read number preventing pipeline from calling variant with TAF, but variant seen on manual curation and validated with dPCR

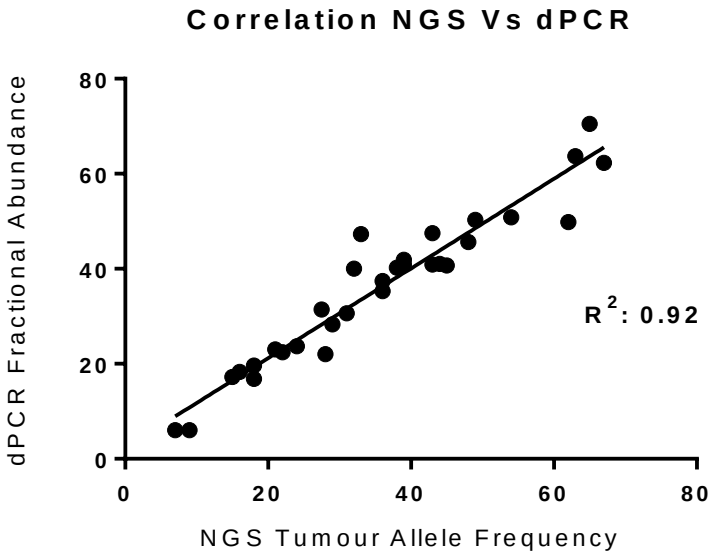

Supplementary Figure 1 – Scatter plot illustrating correlation between NGS and dPC